Induction of visual orientation modules in auditory cortex

Jitendra Sharma, Alessandra Angelucci* & Mriganka Sur

Department of Brain and Cognitive Sciences, Massachusetts Institute of Technology,Cambridge, Massachusetts 02139, USA

Modules of neurons sharing a common property are a basic organizational feature of mammalian sensory cortex. Primary visual cortex (V1) is characterized by orientation modules—groups of cells that share a preferred stimulus orientation—which are organized into a highly ordered orientation map. Here we show that in ferrets in which retinal projections are routed into the auditory pathway, visually responsive neurons in 'rewired' primary auditory cortex are also organized into orientation modules. The orientation tuning of neurons within these modules is comparable to the tuning of cells in V1 but the orientation map is less orderly. Horizontal connections in rewired cortex are more patchy and periodic than connections in normal auditory cortex, but less so than connections in V1. These data show that afferent activity has a profound influence on diverse components of cortical circuitry, including thalamocortical and local intracortical connections, which are involved in the generation of orientation tuning, and long-range horizontal connections, which are important in creating an orientation map.

Whether activity in sensory pathways has a specific, instructive role in the development of cortical networks is unclear[1,2]. Much of the evidence for or against an instructive influence of activity on cortical development derives from experiments in the visual cortex that have examined two kinds of columnar structure—ocular dominance columns and orientation columns. Ocular dominance columns arise from the segregation of inputs from eye-specific layers of the lateral geniculate nucleus: although visual deprivation can alter the size of these columns[3], they can develop even in the absence of retinal inputs from an early stage of development[4], and hence appear not to require instructive, patterned activity from the retina for their establishment.

Orientation columns represent a more complex network, involving both thalamocortical and local intracortical connections, which generate orientation selectivity[5,6], and long-range horizontal connections, which preferentially link cortical columns of like orientation[7]. Several lines of evidence have been taken to indicate that orientation maps in visual cortex rely on an intrinsic scaffold of connections that are influenced little by activity[8–11]. These studies are complicated by two factors[12]. First, the manipulation commonly employed to study the role of activity—visual deprivation—reduces afferent activity nonspecifically and cannot provide information on an instructive role for patterned activity. Second, many of these manipulations start late in development, commonly after some orientation selectivity and an orientation map are already established, and hence address the role of activity in the maintenance of orientation columns rather than their emergence.

We reasoned that presenting patterned activity—visual inputs—to a cortex with a radically different organization of horizontal connections from V1, at a very early stage in cortical development (before thalamic innervation of the cortical plate and well before horizontal connections start to grow or cluster), would allow us to investigate clearly whether afferent activity or intrinsic features of the cortical target regulate the development of orientation columns. We routed fibres from the retina to the auditory pathway in ferrets[13], to cause visual activation of auditory cortex without altering thalamocortical connections. Here we show that, within limits, input activity has a significant instructive role in establishing the cortical circuits that underlie orientation selectivity and the orientation map.

Deafferentation of the auditory thalamus in ferrets at birth induces retinal axons to innervate the medial geniculate nucleus (MGN)[14,15]. Visual input is relayed from the retina through the MGN to primary auditory cortex (A1), which develops with a different pattern of input activity than normal A1. A map of visual space arises in rewired A1 (ref. 16), and visually driven cells are orientation selective[17]. We have now asked whether the orientation tuning of cell populations in rewired A1 is comparable to that in V1, whether the rewired cortical cells are organized into an orientation map, and whether horizontal connections in this cortex are shaped by visual activity and underlie the map as they do in V1.

Orientation preference map in rewired cortex

Optical imaging of intrinsic signals in A1 of rewired ferrets (Fig. 1A; $n = 4$ animals) in response to full-field oriented gratings reveals well-defined domains of visual activity (Fig. 1B). Vector averaging of the responses to a full set of stimulus orientations reveals a map with iso-orientation regions, where neurons share the same orientation preference, and singularities, where adjacent stimulus orientations are organized in 'pinwheel' fashion (Fig. 1C). The strength of orientation tuning is reflected in the magnitude of the orientation vector at each pixel, which in general is high in iso-orientation regions and low at and between pinwheel centres (Fig. 1D). We quantified the periodicity of the orientation representation by computing first a two-dimensional autocorrelation function of individual single orientation maps (Fig. 1E), and then a power spectrum by a Fourier transform of the autocorrelation (Fig. 1F). For a disordered and aperiodic map, the autocorrelation would have a peak at zero displacement and little other structure. The power spectrum would have a peak at zero spatial frequency corresponding to the mean power in the autocorrelation, and low, broadly distributed power at other spatial frequencies. For a highly periodic map, the autocorrelation would show peaks at the period cycle, and the power spectrum would show a peak at the cycle frequency[18]. The autocorrelation and power spectrum of the orientation maps in rewired A1 indicate relatively low periodicity in the representation.

In comparison, V1 of normal animals (Fig. 1G; $n = 3$ animals) contains regular domains of activity that respond to stimuli of a single orientation (Fig. 1H). The map of orientation preference shows the orderly distribution of iso-orientation regions and pinwheel centres[19,20] (Fig. 1I and J). The autocorrelation of the V1 map (Fig. 1K) demonstrates the quasi-periodic layout of orientation domains with an average periodicity of about 750 μm (pooling both axes of cortex) and the power spectrum shows a significant peak at a spatial frequency of 1.3 cycle per mm along with harmonics (Fig. 1L).

* Present address: Department of Visual Science, Institute of Ophthalmology, 11–43 Bath Street, London EC1V 9EL, UK.

The orientation map in rewired A1 has similarities to and differences from the map in V1. Although both contain a pinwheel organization, the density of pinwheel centres in rewired A1 (1.1 ± 0.3 per mm^2; four animals) is one-quarter of that in V1 (4.5 ± 0.4 per mm^2; three animals). The maps in V1 and rewired A1 were obtained with binocular stimulation, at a spatial frequency of 0.375 cycle per degree. Neurons in striate cortex are selective for a limited set of spatial frequencies[21]. When gratings of lower spatial frequency (0.175 cycle per degree) were interleaved with the higher spatial frequency gratings (0.375 cycle per degree), the responses were considerably weaker (by a factor of 2) in V1 ($n = 1$ animal) and virtually absent in rewired A1 ($n = 3$ animals; data not shown). No visually driven intrinsic signal activity could be elicited from A1 with a range of spatial and temporal frequencies in two normal, control ferrets.

The reproducibility of the orientation maps from rewired A1 as well as normal V1 was evaluated by summing alternate blocks of trials to construct single orientation maps and composite maps of orientation preference[20]. We then calculated the root mean square (r.m.s.) of the difference between preferred angle for each pixel in the two sets of angle maps. The average r.m.s. angle difference was 8.5° (range: 6.5–9.4°) in the rewired A1 cases and 8.6° (range: 7.2–9.0°) in the V1 cases. To evaluate the stability of the maps, we compared single orientation maps obtained at the beginning of the imaging session (average of 10 trials) with the maps obtained 4–5 h later, at the end of the imaging session. The average r.m.s. difference between the two sets of corresponding single condition maps was less than 8% (range: 6.4–10.8%) for the rewired A1 as well as V1 maps—a value that compares well with similar analyses of visual cortex of cats[22].

We compared the strength of intrinsic signals in rewired A1 and V1 by evaluating the relative change in reflectance, $\delta R/R$, of the stimulated cortex (where R is the reflectance in an unstimulated condition[22]). The average $\delta R/R$ value computed on a pixel-by-pixel basis was 2.9×10^{-3} in rewired A1 ($n = 4$ animals) and 2.3×10^{-3} in normal V1 ($n = 3$ animals). These values are similar to those measured in cat and monkey visual cortex[20,23]. We also calculated the change in the reflected light intensity in the stimulated condition relative to that in the unstimulated condition over the entire map. This was between 2.1% and 3.8% in rewired A1 cases and

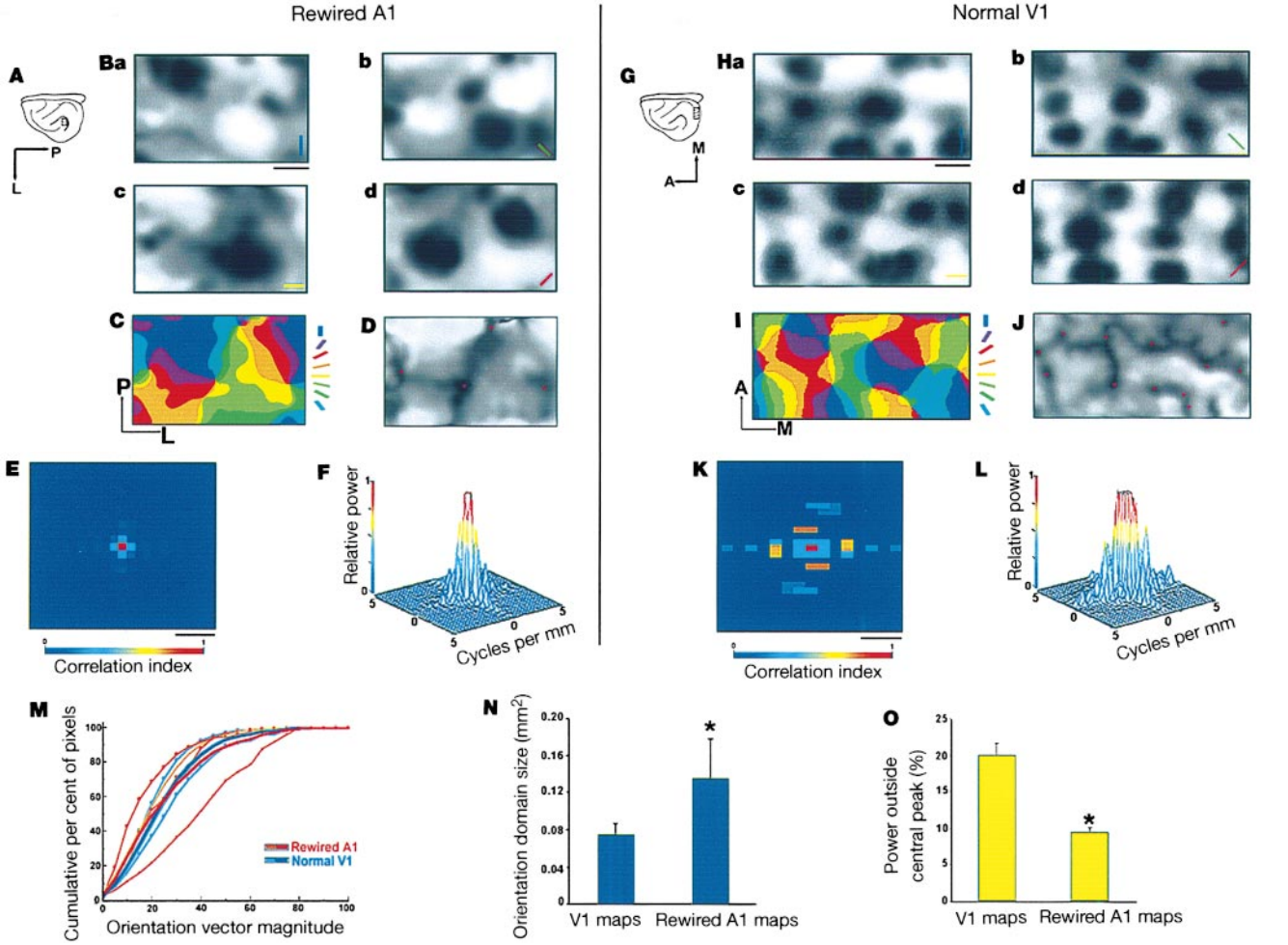

Figure 1 Orientation maps in 'rewired' A1 and normal V1. **A**, Lateral view of a rewired ferret brain showing imaged A1 region (crosshatched). L, lateral; P, posterior: compare with **C** for orienting **B–D**. **Ba–d**, Single orientation maps in response to grating stimuli of different orientations. Dark regions represent high activity. Scale bar, 0.5 mm (for **B–D**). **C**, Composite map of orientation preference. Colour bar, key for representing orientations. **D**, Map of orientation vector magnitude. Dark regions, low vector magnitude; red dots, pinwheel centres. **E**, Two-dimensional autocorrelogram of the single orientation map shown in **Ba**. Colour bar here and in **K** shows the strength of correlation. Scale bar, 1 mm. **F**, Power spectrum computed by a two-dimensional Fourier transform of **E**. **G**, Lateral view of a normal ferret brain showing imaged V1 region (crosshatched). A, anterior; M, medial: compare with **I** for orienting **H–J**. **Ha–d** and **I–L** are parallel results from normal ferret V1 and follow the same order as in **Ba–d**, **C–F**. **M**, Cumulative histogram of normalized orientation vector magnitudes for V1 cases (in blue, $n = 3$) and rewired A1 cases (in red, $n = 4$). Light traces show data from individual animals, dark traces show the mean. **N**, Domain sizes from single orientation maps in V1 and rewired A1. Asterisk, $P < 0.05$, Mann–Whitney U-test. **O**, Comparison of non-DC power in V1 and rewired A1 maps.

between 1.8% and 2.6% in normal V1 cases (compare with ref. 23 for monkey visual cortex). As the signal change and $\delta R/R$ values were comparable in normal V1 and rewired A1, we compared the orientation vector magnitudes of pixels across the individual cases. There is no difference in the strength of orientation tuning of pixels in rewired A1 and normal V1 (Fig. 1M): the average cumulative magnitude plots are nearly identical for the two cortices ($P > 0.9$, Kolmogorov–Smirnov test). However, as apparent from the single orientation maps (Fig. 1B and H), the size of orientation domains in rewired A1 is significantly larger than that in V1 (Fig. 1N; $P < 0.05$, Mann–Whitney *U*-test, treating each animal as a single datum). The domains are also organized less periodically in rewired A1, for there is less power at non-zero spatial frequencies in the rewired A1 maps compared to the V1 maps (Fig. 1O; $P < 0.01$, Mann–Whitney *U*-test).

Orientation tuning in rewired A1 and AF

To compare the orientation tuning of cells in rewired cortex and normal V1 further, we combined optical imaging with single-unit recording at several sites in the cortex. Figure 2a and b shows the orientation map in a rewired ferret over an expanse of cortex that includes A1 and the anterior field (AF)[24], a cortical area that receives thalamocortical input from auditory thalamic nuclei that also innervate A1 (ref. 25) as well as corticocortical input from A1 (refs 26–28). The map in rewired AF has features typical of rewired A1 orientation maps, that is, a low density of pinwheels and relatively large orientation domains that are less periodically distributed than the orientation map in V1. The imaged map (Fig. 2b) has a discontinuity at the border between A1 and AF owing to a dense network of blood vessels emanating from the pseudosylvian sulcus, which swamps the optical signal.

After imaging, we recorded from cells in the superficial layers of rewired A1 and AF. The orientation preference of these cells was consistent with the orientation domain in which they were located (Fig. 2b), matching the orientation domain within ±22.5° (Pearson's correlation coefficient $r = 0.86$, $P < 0.001$, $n = 42$ cells

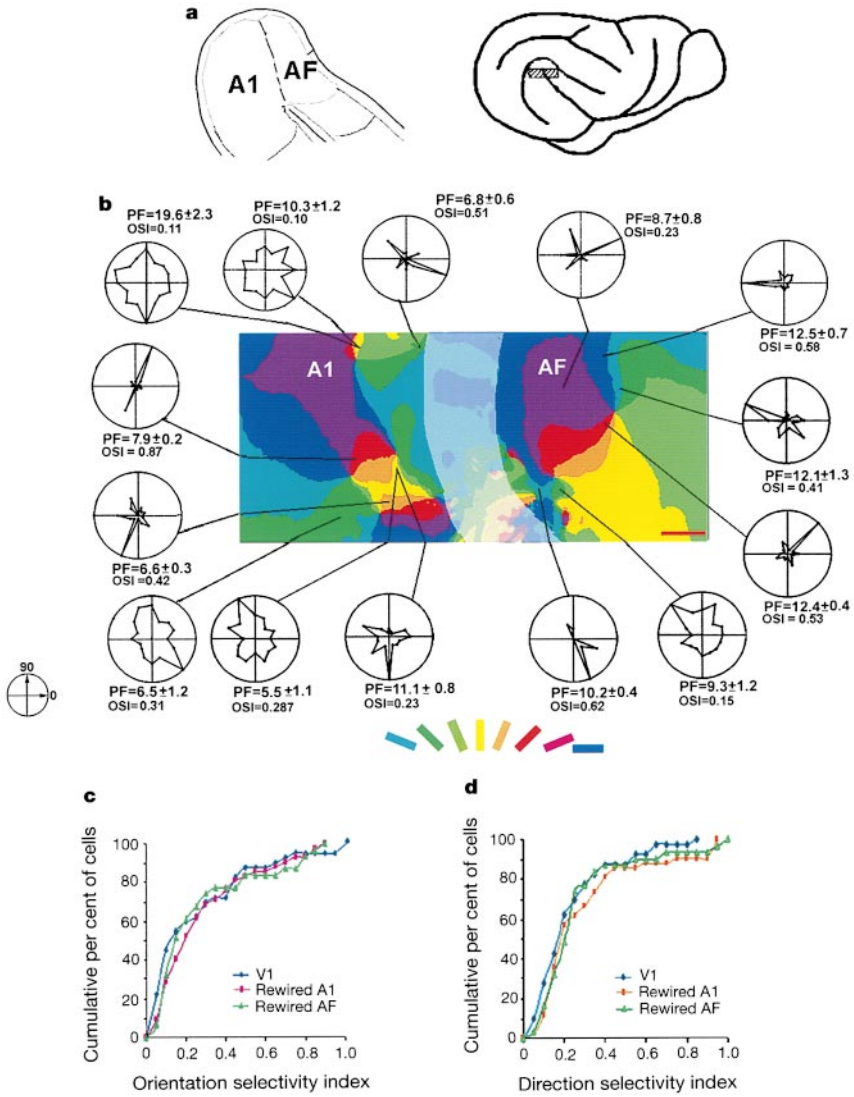

Figure 2 Optically imaged orientation maps and single cell responses in rewired ferret auditory cortex. **a**, Right, lateral view of a ferret brain showing the imaged area (crosshatched) straddling anterior auditory field (AF) and A1; left, expanded view of the two cortical fields. This is a different animal than the case shown in Fig. 1A–D. **b**, Orientation map in A1 and AF showing a systematic arrangement of orientation domains in both regions (the grey band in the centre denotes a thick plexus of blood vessels straddling the approximate boundary between A1 and AF). The location of single cells recorded in the same cortex following optical imaging is shown, along with their polar plots (OSI, orientation selectivity index; PF, peak firing rate ± s.d. at the preferred orientation for individual cells). Some recordings were made at two depths within the same penetration. **c**, Cumulative histogram of the OSI of cells in normal ferret V1, rewired A1 and rewired AF. **d**, Cumulative histogram of the direction selectivity index of cells in normal V1, rewired A1 and rewired AF.

in rewired A1; $r = 0.92$, $P < 0.001$, $n = 31$ cells in rewired AF). An analysis of V1 cells in relation to their orientation map (data not shown) showed a similar match ($r = 0.90$, $P < 0.001$, $n = 48$ cells). The visual response levels of cells recorded in rewired A1 and AF and those in normal V1 were similar (max/min/mean firing rates in spikes s^{-1} were: rewired A1, 37.8/4.5/13.67, $n = 42$; rewired AF, 35.5/4.1/13.9, $n = 31$; normal V1, 42/4.5/14.15, $n = 48$; $P > 0.5$ for all pairwise comparisons, Mann–Whitney *U*-test). We calculated an orientation selectivity index (OSI) for cells as a measure of the strength of orientation tuning, in a manner identical to the calculation of the orientation vector magnitude of pixels in the orientation maps (see Methods). The OSIs (Fig. 2c) of cells in rewired A1 and AF, and in V1, were similar ($P > 0.5$ for all pairwise comparisons; Kolmogorov–Smirnov test). We also calculated a direction selectivity index (DSI) for cells as a measure of their strength of direction tuning (see Methods). The DSI distributions for the three areas (Fig. 2d) were also statistically indistinguishable ($P > 0.5$). Orientation and direction selective responses from rewired A1 and AF indicate the creation of emergent response properties in multiple cortical areas that receive novel visual input, in a manner analogous to the responses of neurons in visual cortical areas V1 and V2. The close correspondence between the OSI distributions of cells and the orientation vector magnitude distributions of pixels in rewired A1 and normal V1 shows that orientation tuning is very similar in the two cortical areas.

Horizontal connections and orientation maps

Because the organization of cells into an orientation map in rewired A1 is less orderly than that in V1 (Fig. 1), we examined the anatomical substrate of the map by defining the clustering and periodicity of long-range horizontal connections within the superficial layers of V1 and rewired A1. We also compared the connections in normal A1. A focal injection of cholera toxin B (CTB) in the superficial layers of V1 ($n = 6$ animals) defines a field of retrogradely labelled cells that is very patchy and elongated mediolaterally (parallel to the V1–V2 border; Fig 3a). In contrast, a similar injection in normal A1 ($n = 3$ animals) leads to a band-like pattern of retrogradely labelled cells that is also anisotropic, but elongated anteroposteriorly along the isofrequency axis of A1 (refs 28, 29) (Fig. 3b). Peaks in cell densities are often seen within the main labelled 'band', and in some cases (not shown), occasional satellite patches lie off the main isofrequency axis. Retrogradely labelled cells in rewired A1 form a patchy and anisotropic distribution around the injection site, but similar to the connections in V1, the labelled field's longest axis is elongated mediolaterally, that is, orthogonal to the isofrequency axis of A1, and sparser cells are seen between patches (Fig. 3c). The maximal linear dimension of the labelled field in cortex, based on similar sized injections, is larger in V1 ($4.8 \pm 0.08 \times 1.7 \pm 0.2$ mm) than in normal A1 ($3.2 \pm 0.26 \times 2.4 \pm 0.27$ mm; $P < 0.05$, Student's *t*-test), whereas the extent in rewired A1 ($4 \pm 1.45 \times 2.9 \pm 0.64$ mm) is intermediate and not significantly different from either area (Fig. 3d). However, the ratio of the anteroposterior extent of label to its mediolateral extent is significantly lower in rewired A1 (ref. 30) than in normal A1 (Fig. 3e; $P < 0.05$, Mann–Whitney *U*-test), indicating that the connectional field in rewired A1 is anisotropic along the mediolateral axis, as it is in V1.

We examined the detailed distribution of cells in each area by

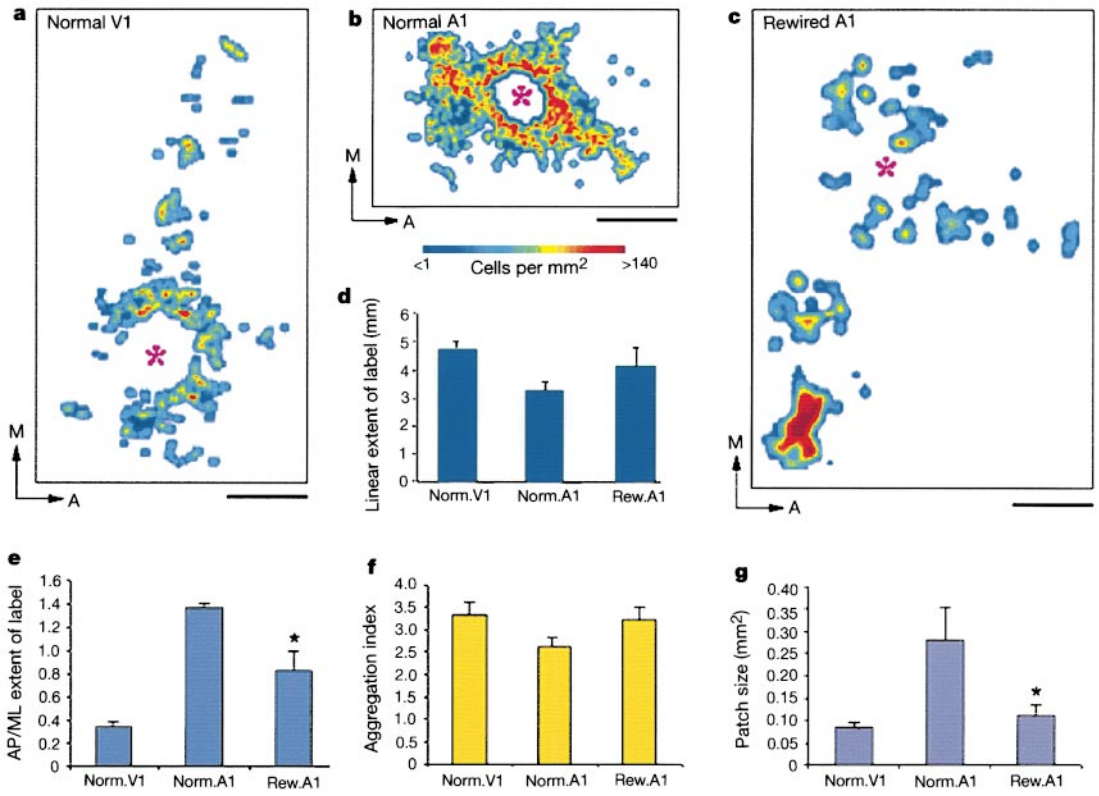

Figure 3 Patterns of long-range horizontal connections in V1, normal A1 and rewired A1. **a–c**, Cell density distribution maps obtained from single injections of CTB in normal V1 (**a**), normal A1 (**b**) and rewired A1 (**c**). Colour bar under **b** shows the density distribution ranging from <1 cell per mm^2 to >140 cells per mm^2, and applies to **a** and **c** as well. Asterisk, injection site; A, anterior; M, medial. Scale bars (**a–c**), 500 μm. **d**, Histogram of the extent of the overall labelled field's long axis in V1, normal A1 and rewired A1. **e**, Histogram of the ratio of anterioposterior extent of label to its mediolateral extent in V1, normal A1 and rewired A1. **f**, Histogram of cell aggregation index (see Methods) in V1, normal A1 and rewired A1. **g**, Histogram of the area of labelled cell patches in V1, normal A1 and rewired A1. Asterisk, $P < 0.05$, Mann–Whitney *U*-test comparing rewired A1 and normal A1.

calculating an index of cell aggregation[10,31] (see Methods), and by defining cell patches and measuring their sizes. The aggregation index provides a measure of the extent to which cells are clumped into patches or are randomly distributed within the overall matrix of labelled cells. The index is higher in V1 than in normal A1 (Fig. 3f; $P < 0.05$, Mann–Whitney U-test), whereas the index in rewired A1 is intermediate and not significantly different from either area ($P > 0.1$). The number of patches resulting from single CTB injections in rewired A1 (mean, 12 ± 1) is similar to that in V1 (mean, 12 ± 2), and considerably greater than that in normal A1 (mean, 4 ± 1; $P < 0.05$, Mann–Whitney U-test). The size of patches in rewired A1 (Fig. 3g) is larger on average than in V1 ($P < 0.1$, Student's t-test), but smaller than in normal A1 ($P < 0.01$). Thus, as in V1, long-range intrinsic connections in rewired A1 form multiple patches that spread mediolaterally in cortex. However, the patches tend to be larger in rewired A1 than in V1, resembling the optically imaged domains in response to single stimulus orientations (Fig. 1N).

To ascertain the correspondence between intrinsic connections and orientation maps, we made CTB injections at the end of optical imaging sessions at specific sites in the cortex, typically in an orientation domain identified in a single orientation map. Figure 4a and b shows the overlay of retrogradely labelled cell patches along with the injection site on single orientation maps obtained in V1 and rewired A1, respectively. For each animal, we calculated the correlation coefficients between the anatomically defined cell distribution and the full set of physiologically imaged single orientation maps. There was significantly higher correlation between cell distributions and orientation maps when the overlap between the injection site (including its dense labelled halo of about 200 μm in diameter) and orientation domain was greater than 90% (the iso-orientation condition), compared to the case when this overlap was less than 50% (V1: $r = 0.73$ for the iso-orientation condition; $r = 0.44$ for other conditions; $n = 8$ maps. Rewired A1: $r = 0.62$ for the iso-orientation condition; $r = 0.47$ for the other conditions; $n = 4$ maps; $P < 0.05$, Mann–Whitney U-test, comparing iso- and other conditions). Thus, in both V1 and rewired A1, intrinsic horizontal connections preferentially link regions that map similar orientations.

We next examined the periodicity of intrinsic connections in rewired A1 and compared it to V1 and normal A1. Figure 5a–c shows the autocorrelation functions and power spectra of the retrogradely labelled cell distributions shown in Fig. 3a–c, respectively. As expected from the cell distributions, the V1 autocorrelation shows periodicity in the mediolateral dimension with a cycle of 500–750 μm, the normal A1 autocorrelation shows little periodicity, and the rewired A1 autocorrelation shows a mediolaterally extended and partially periodic distribution with multiple cycles. As shown for the orientation maps in rewired A1 and V1 (Fig. 1O), the non-zero power in the power spectra provides a means of comparing the periodicities of cell distributions in the three cortices (Fig. 4d). This power is significantly higher in V1 cases compared to rewired A1, which in turn is significantly higher than in normal A1 ($P < 0.05$, Mann–Whitney U-test for each comparison).

Together, these data show that the routing of visual inputs to auditory cortex leads to: (1) sharp orientation selectivity in rewired A1, with the tuning of individual cells and of optically imaged pixels comparable to that in normal V1; (2) orientation maps in rewired A1 that contain a systematic arrangement of iso-orientation domains, although the domains are larger and the map shows less order than in V1; (3) long-range horizontal connections in rewired A1 with smaller patches that are more numerous and more periodically distributed than connections in normal A1, but are larger and less periodic than in V1. Furthermore, horizontal connections in rewired A1 resemble V1 connections in their mediolateral anisotropy.

Discussion

Normally, in V1 of carnivores and primates, sharp orientation tuning coexists with a highly ordered orientation map. Sharp orientation tuning coupled with a less orderly map in rewired A1 indicates that these two features are independent, and that, more

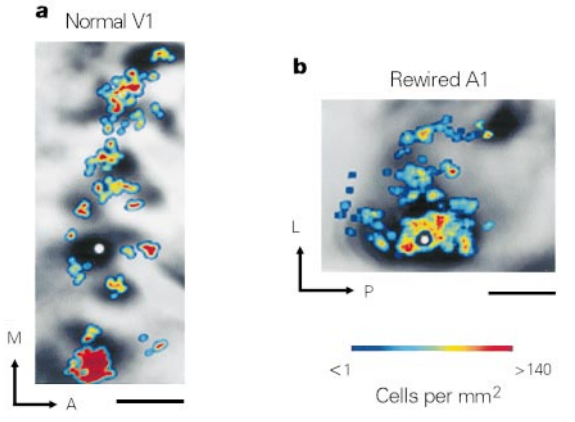

Figure 4 Correlation of optical imaging maps with intrinsic horizontal connections in normal V1 and rewired A1. **a**, Overlay of the cell density distribution on a single orientation map (responding to a grating of 45° orientation) in V1 of a normal ferret. The map is from a different case than that shown in Fig. 1G–J. The injection site (white dot) is within an imaged domain. The majority of labelled cell patches lie inside or close to the domains of the same orientation (dark areas). Scale bar, 0.5 mm. **b.** Cell patches overlaid on a single orientation map (in response to a grating of 135°) in rewired A1. This map is from a different case than those shown in Figs 1A–D and 2b. The injection site (white dot) is within an imaged domain. Scale bar, 0.5 mm. Colour bar shows cell density per mm^2. In both the normal V1 and rewired A1 case, the cell distribution shows a significant correlation with the domains of the underlying optical map and is less correlated with other single orientation maps, indicating that iso-orientation domains in normal V1 and in rewired A1 are preferentially interconnected by the pattern of horizontal connections.

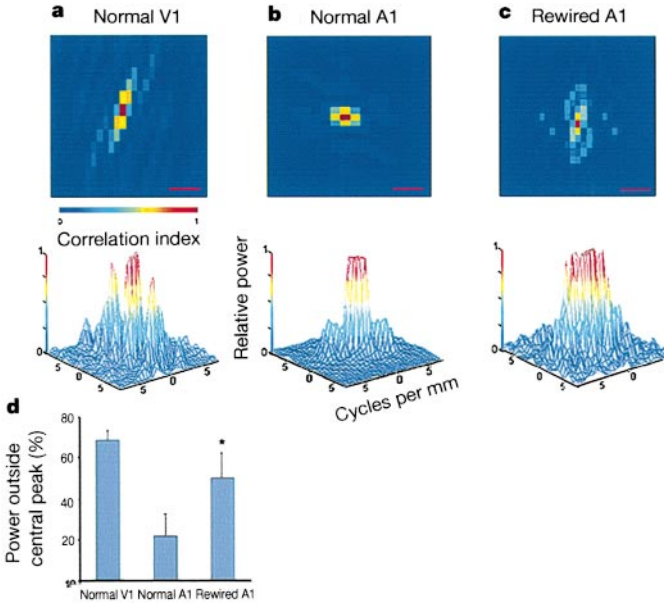

Figure 5 The periodicity of horizontal connections in normal V1, normal A1 and rewired A1. **a–c**, Top, two-dimensional autocorrelograms of the cell distributions shown in Fig. 3 (a–c). Scale bar, 1mm; colour bar underneath **a** shows the strength of correlation in all plots. Bottom, power spectrum of the cell distributions computed by a Fourier transform of the respective autocorrelograms. **d**, The non-DC power in the power spectrum is significantly higher in rewired A1 than in normal A1 (asterisk), indicating more periodic horizontal connections in rewired A1.

generally, the form of a cortical map may be dissociated from the mapped variable. A result complementary to ours is provided by artificial stimulation of the optic nerve in ferrets, which leads to poorly tuned cells in V1 but an orientation map that is indistinguishable from normal[32]; an important caveat, however, is that the stimulation was initiated late in development and the stimulation paradigm might have been too nonspecific to be disruptive[33]. Orientation tuning is thought to be generated by a bias in the feedforward thalamocortical inputs that is then amplified by recurrent excitatory networks in cortex[6]. Orientation tuning of V1 neurons arises early in development[34], though late manipulations including lid suture[34], intracortical blockade of activity[34], artificial stimulation of the optic nerve[32] and stripe rearing[35] can all reduce or alter orientation selectivity. These experiments indicate that afferent activity is required for at least the maintenance of orientation selectivity in V1 neurons. Our experiments routed visual activity to auditory cortex at an extremely early stage in cortical development, when thalamocortical axons are still waiting in the subplate[12]. Thus, they indicate an instructive role for patterned activity in establishing sharp orientation selectivity even in a novel cortex, and in multiple cortical areas such as rewired A1 and AF.

The orientation map in V1 might arise by clustering of horizontal connections that preferentially link iso-orientation domains[7,36,37], is also established early[38], and is resistant to later manipulations of afferent activity. In particular, reverse suture[8] and alternating lid suture[9] lead to precisely matched orientation maps from the two eyes, leading to the proposal that the map relies on an intrinsic scaffold of horizontal connections in V1. However, horizontal connections in V1 can be subtly altered by input correlations: whereas these connections in normal cats do not respect ocular dominance columns, artificial strabismus causes horizontal connections to link columns of the same eye[39] and orientation preference[40]. Our results show, for the first time, that the pattern of thalamocortical activity alone, routed early and without altering thalamocortical connections, can significantly shape horizontal connections and create an orientation map in rewired A1. We demonstrate, using a combination of techniques, the close correspondence between the functional cortical network of orientation selectivity and the underlying anatomical structure. The differences between orientation maps and horizontal connections in rewired A1 and in V1 suggest constraints on activity-dependent plasticity. However, there are important similarities between the two areas, which is remarkable given that most retinal input to rewired A1 arises from W cells, whereas that to V1 arises from X and Y cells (ref. 41; but see ref. 15). Together with the demonstration that the visual projection routed to auditory cortex mediates visual behaviour and hence instructs the perceptual modality of cortex[42], our findings show that the pattern of early sensory activation can instruct the functional architecture of cortex to a significant extent. □

Methods

We used 17 adult pigmented ferrets. Six of these received neonatal brain lesions to route retinal axons to the MGN; the rest were used as normal controls. All experiments were performed under protocols that were approved by MIT's Institutional Animal Care and Use Committee and conformed to NIH guidelines.

Neonatal surgery

Ferret kits born of timed-pregnant mothers (Marshall Farms) received bilateral brain lesions one day after birth to route retinal axons to the MGN. The MGN was deafferented and the superior colliculus was ablated, as described[15]. Animals were reared to adulthood before being used in further experiments.

Optical imaging of intrinsic signals

Techniques for intrinsic signal imaging were similar to those described previously[19,20]. Either the ectosylvian gyrus (A1) or the occipital pole (V1) was exposed. Binocularly presented visual stimuli consisted of full-field square wave gratings (0.375 cycle per degree drifted at 1.0 Hz or 0.175 cycle per degree drifted at 1.5 Hz), presented at four or eight different orientations and drifted in two opposite directions. The optical signal was acquired with an imaging system (Optical Imaging) and analysed using in-house programs. Spatial layouts of the normal V1 and rewired A1 maps were compared by performing a two-dimensional autocorrelogram of the single orientation maps followed by a two-dimensional Fourier transform[18] of the autocorrelogram to compute the power spectrum. Non-DC power in the power spectrum was calculated by subtracting the central 5×5 pixel values from the total power. Orientation vector magnitudes were calculated by summing vectorially the signal values for the single orientation maps on a pixel-by-pixel basis. As $\delta R/R$ and signal changes among orientation maps across different animals were comparable (see text), the magnitudes were normalized for comparison across cases.

Single-unit recording

We used an array of four parylene-coated tungsten microelectrodes (FHC Instruments). Computer-generated visual stimuli were the same as those used for optical imaging, and were presented 10–15 times pseudo-randomly. The locations of electrode penetrations were marked on the superficial blood vessel image of the cortex, which was used as a reference for alignment of recording sites with the optical maps. The spike waveforms from individual cells were sorted and analysed off-line into single neuron records (Datawave). Orientation and direction selectivity indices (OSI and DSI, respectively) were calculated as the second and first Fourier transforms of spike responses respectively, which is identical to vector averaging of responses from imaged pixels[43], and scaled from 0–1.

Labelling of horizontal connections

Focal injections of the anatomical tracer cholera toxin subunit B (CTB, 2% in 0.1 M phosphate buffer, pH 6.0) were made iontophoretically (2 μA, 7–15 min; pipette inner tip diameter, 7–17 μm) in V1, normal A1 and rewired A1 at a depth of 250–300 μm below the cortical surface. WGA–HRP (2% in saline, 1 μl) was pressure injected in an additional rewired ferret. In optically imaged animals, fiducial marks were made in the cortex for aligning the images with cell distributions. At the end of the survival period (20 h–2 days), animals were euthanized and perfused transcardially, and the brains cut in tangential sections (40–50 μm) and processed[44]. Retrogradely labelled cells in tissue sections were drawn under camera lucida, and adjacent sections superimposed using the vasculature pattern for alignment.

The cell density distribution was determined by a window smoothing method[37]. Patch size was defined as the area contained within the 33rd percentile of the density distribution. To quantify the degree of cell clustering within the labelled fields, we calculated an Aggregation Index derived from Hopkins' statistics for spatial randomness[31]. In a random distribution, the ratio $\Sigma(\beta^2)/\Sigma(\alpha^2)$, where α is mean distance between nearest-neighbours and β is distance between a random point and the closest data point, equals 1, whereas a ratio >1 shows increasing aggregation among data points. Values were averaged over 10 repetitions of a window of 50×50 pixels scanned over the entire region of interest, and the median value was taken as the Aggregation Index. Autocorrelograms and power spectra of the cell distributions were computed as for the optically imaged maps. To exclude contributions from local short-range connections, all quantitative analyses of anatomical data excluded the region of intense and uniform cell label surrounding the injection.

Received 30 December 1999; accepted 23 February 2000.

1. Katz, L. C. & Shatz, C. J. Synaptic activity and the construction of cortical circuits. *Science* **274,** 1133–1138 (1996).
2. Yuste, R. & Sur, M. Development and plasticity of the cerebral cortex: from molecules to maps. *J. Neurobiol.* **41,** 1–6 (1999).
3. Shatz, C. J. & Stryker, M. P. Ocular dominance in layer IV of the cat's visual cortex and the effects of monocular deprivation. *J. Physiol.* **281,** 267–283 (1978).
4. Crowley & Katz, L. C. Development of ocular dominance columns in the absence of retinal input. *Nature Neurosci.* **2,** 1125–1130 (1999).
5. Ferster, D., Chung, S. & Wheat, H. Orientation selectivity of thalamic input to simple cells of cat visual cortex. *Nature* **380,** 249–252 (1996).
6. Somers, D. C., Nelson, S. B. & Sur, M. An emergent model of orientation selectivity in cat visual cortical simple cells. *J. Neurosci.* **15,** 5448–5465 (1995).
7. Gilbert, C. D. & Wiesel, T. N. Columnar specificity of intrinsic horizontal and corticocortical connections in cat visual cortex. *J. Neurosci.* **9,** 2432–2442 (1989).
8. Kim, D.-S. & Bonhoeffer, T. Reverse occlusion leads to a precise restoration of orientation preference maps in visual cortex. *Nature* **370,** 370–372 (1994).
9. Godecke, I. & Bonhoeffer, T. Development of identical orientation maps for two eyes without common visual experience. *Nature* **379,** 251–254 (1996).
10. Ruthazer, E. & Stryker, M. P. The role of activity in development of long range horizontal connections in area 17 of the ferret. *J. Neurosci.* **16,** 7253–7269 (1996).
11. Crair, M. C., Gillespie, D. C. & Stryker, M. P. The role of visual experience in the development of columns in cat visual cortex. *Science* **279,** 566–570 (1998).
12. Sur, M., Angelucci, A. & Sharma, J. Rewiring cortex: The role of patterned activity in development and plasticity of neuronal circuits. *J. Neurobiol.* **41,** 33–43 (1999).
13. Sur, M., Garraghty, P. E. & Roe, A. W. Experimentally induced visual projections into auditory thalamus and cortex. *Science* **242,** 1437–1441 (1988).
14. Angelucci, A., Clasca, F., Bricolo, E., Cramer, K. S. & Sur, M. Experimentally induced retinal projections to the ferret auditory thalamus: development of clustered eye-specific patterns in a novel target. *J. Neurosci.* **17,** 2040–2055 (1997).
15. Angelucci, A., Clascá, F. & Sur, M. Brainstem inputs to the ferret medial geniculate nucleus and the effect of early deafferentation on novel retinal projections to the auditory thalamus. *J. Comp. Neurol.* **400,** 417–439 (1998).
16. Roe, A. W., Pallas, S. L., Hahm J.-O. & Sur, M. A map of visual cortex induced in primary auditory cortex. *Science* **250,** 818–820 (1990).
17. Roe, A. W., Pallas, S. L., Kwon, Y. H. & Sur, M. Visual projections routed to the auditory pathway in

ferrets: receptive fields of visual neurons in the primary auditory cortex. *J. Neurosci.* **12,** 3651–3664 (1992).
18. Oppenheim, A. V. & Schafer, R. W. *Digital Signal Processing* (Prentice–Hall, New Jersey, 1975).
19. Rao, S. C., Toth, L. J. & Sur, M. Optically imaged maps of orientation preference in primary visual cortex of cats and ferrets. *J. Comp. Neurol.* **387,** 358–370 (1997).
20. Bonhoeffer, T. & Grinvald, A. The layout of iso-orientation domains in area 18 of cat visual cortex: optical imaging reveals a pinwheel-like organization. *J. Neurosci.* **13,** 4157–80 (1993).
21. Tolhurst, D. J. & Thompson, I. D. On the variety of spatial frequency selectivities shown by neurons in the area 17 of cat. *Proc. R. Soc. Lond. B* **213,** 183–199 (1981).
22. Bonhoeffer, T. & Grinvald, A. in *Brain Mapping: The Methods* (eds Toga, A. W. & Mazziotta, J. C.) (Academic, New York, 1996).
23. Frostig, R. D., Lieke, E. E., Ts'o, D. Y. & Grinvald, A. Cortical functional architecture and local coupling between neuronal activity and the microcirculation revealed by *in vivo* high resolution optical imaging of intrinsic signals. *Proc. Natl Acad. Sci. USA* **87,** 6082–6086 (1990).
24. Kowalski, N., Versnel, H. & Shamma, S. A. Comparison of responses in the anterior and primary auditory fields of the ferret cortex. *J. Neurophysiol.* **73,** 1513–1520 (1995).
25. Andersen, R. A., Knight, P. L. & Merzenich, M. M. The thalamocortical and corticothalamic connections of AI, AII, and the anterior auditory field (AAF) in the cat: evidence for two largely segregated systems of connections. *J. Comp. Neurol.* **194,** 663–701 (1980).
26. Imig, T. J. & Reale, R. A. Patterns of cortico-cortical connections related tonotopic maps in cat auditory cortex. *J. Comp. Neurol.* **192,** 293–332 (1980).
27. Pallas, S. L. & Sur, M. Visual projections induced into the auditory pathway of ferrets. II. Cortico-cortical connections of primary auditory cortex. *J. Comp. Neurol.* **336,** 317–333 (1993).
28. Wallace, M. N., Kitzes, L. M. & Jones, E. G. Intrinsic inter- and intralaminar connections and their relationship to the tonotopic map in cat primary auditory cortex. *Exp. Brain Res.* **86,** 527–544 (1991).
29. Matsubara, J. A. & Phillips, D. P. Intracortical connections and their physiological correlates in the primary auditory cortex (AI) of the cat. *J. Comp. Neurol.* **268,** 38–48 (1988).
30. Gao, W. & Pallas, S. L. Cross-modal reorganization of horizontal connectivity in auditory cortex without altering thalamocortical projections. *J. Neurosci.* **19,** 7940–7950 (1999).
31. Hopkins, B. A new method for determining the type of distribution of plant individuals. *Ann. Botany N. S.* **18,** 213–227 (1954).
32. Weliky, M & Katz, L. C. Disruption of orientation tuning in visual cortex by artificially correlated neuronal activity. *Nature* **386,** 680–685 (1997).
33. Goodhill, G. J. Stimulating issues in cortical map development. *Trends Neurosci.* **20,** 375–376 (1997).
34. Chapman, B. & Stryker, M. P. Development of orientation selectivity in ferret visual cortex and effects of deprivation. *J. Neurosci.* **13,** 5251–5262 (1993).
35. Sengpiel, F., Stawinski, P. & Bonhoeffer, T. Influence of experience on orientation maps in cat visual cortex. *Nature Neurosci.* **2,** 727–732 (1999).
36. Sharma, J, Angelucci, A., Rao, S. C. & Sur, M. Relationship of intrinsic connections to orientation maps in ferret primary visual cortex: iso-orientation domains and singularities. *Soc. Neurosci. Abstr.* **21,** 392 (1995).
37. Callaway, E. M. & Katz, L. C. Effects of binocular deprivation on the development of clustered horizontal connections in cat striate cortex. *Proc. Natl Acad. Sci. USA* **88,** 745–749 (1991).
38. Chapman, B., Stryker, M. P. & Bonhoeffer, T. Development of orientation preference maps in ferret primary visual cortex. *J. Neurosci.* **16,** 6443–6453 (1996).
39. Lowel, S. & Singer, W. Selection of intrinsic horizontal connections in the visual cortex by correlated neuronal activity. *Science* **255,** 209–211 (1992).
40. Schmidt, K. E, Kim, D.-S., Singer, W., Bonhoeffer, T. & Lowel, S. Functional specificity of long-range intrinsic and interhemispheric connections in the visual cortex of strabismic cats. *J Neurosci.* **17,** 5480–5492 (1997)
41. Roe, A. W., Garraghty, P. E., Esguerra, M. & Sur, M. Experimetally induced visual projections to the auditory thalamus in ferrets: evidence for a W cell pathway. *J. Comp. Neurol.* **334,** 263–280 (1993).
42. von Melchner, L., Pallas, S. L. & Sur, M. Visual behaviour mediated by retinal projections directed to the auditory pathway. *Nature* **404,** 871–876 (2000).
43. Worgotter, F. & Eysel, U. T. Quantitative determination of orientational and directional components in response to visual cortical cells to moving stimuli. *Biol. Cybern.* **57,** 349–355 (1987).
44. Angelucci, A., Clascá, F. & Sur, M. Anterograde axonal tracing with the subunit B of cholera toxin: a highly sensitive immunohistochemical protocol for revealing fine axonal morphology in ault and neonatal brains. *J. Neurosci. Methods* **65,** 101–112 (1996).

Acknowledgements

We thank C. Rao and B. Sheth for participating in early experiments; G. Kalarickal for help in aggregation index calculations; J. Schummers for help with matlab; C. Leamey for an injection case; T. McHugh for technical assistance; R. Marini for veterinary care; and C. Moore, C. Hohnke, A. Lykman, V. Dragoi and C. Rivadulla for comments on the manuscript. We also thank T. Bonhoeffer and S. Lowel for being instrumental in initiating this work. Supported by grants from the NIH (M.S).

Correspondence and requests for materials should be addressed to M.S. (e-mail: msur@ai.mit.edu).